Packaging Technology and Science

WILEY

Packaging Technology and Science
An International Journal

RESEARCH ARTICLE OPEN ACCESS

Optimization of Microfibrillated and Nanofibrillated Cellulose Coating to Improve Performance of Paperboard Intended for Food Packaging Applications

Andrea Feroce[1] | Fabio Licciardello[1,2] | Luciano Piergiovanni[3]

[1]Department of Life Sciences, University of Modena and Reggio Emilia, Reggio Emilia, Italy | [2]Interdepartmental Research Centre for the Improvement of Agro-Food Biological Resources (BIOGEST-SITEIA), University of Modena and Reggio Emilia, Reggio Emilia, Italy | [3]CLS Providentia SRL - Social Enterprise, Saronno, Italy

Correspondence: Andrea Feroce (andrea.feroce@unimore.it)

Received: 28 May 2025 | **Revised:** 4 July 2025 | **Accepted:** 24 July 2025

Funding: The authors received no specific funding for this work.

Keywords: bar coating | coating optimization (DOE) | grease resistance | hydrocarbons mineral oils | MFC/NFC | paperboard | spray coating

ABSTRACT

Paper and paperboards represent about 31% of the global food packaging market. However, they show some limits and critical issues (migration of Mineral Oil Hydrocarbons-MOH, poor barrier towards gas, water and grease, no sealability). To overcome these limits, they are often coupled with synthetic polymers, but there is growing interest in the use of natural and biobased coatings. Given the interest in using sustainable processes and recyclable, biodegradable and/or compostable materials, this study aims to optimize the application method of a biobased coating made up of water suspension of micro/nano cellulose fibrils together with some natural functional ingredients. A cellulose-rich biomass was subjected to various high-pressure homogenization cycles and properly formulated. The coating suspension was characterized for pH, dynamic viscosity, dry matter content, ratio between micro and nano fibrils; moreover, dynamic light scattering (DLS) measurements, FTIR and TEM observation were also carried out. The optimization of the paperboard coating process was based on a factorial design with three levels and two factors for each of the two coating methods selected (bar coating and spray coating). The coated paperboards were evaluated for coating grammage, grease resistance (Kit test) and heptane vapour transmission rate (HVTR). On the best conditions selected from both experimental designs water absorption (Cobb Test), water and castor oil contact angle, water vapour transmission rate (WVTR) and surface morphology (SEM and AFM observations) were tested. The results showed that low grammage ($< 10\,g\,m^{-2}$) guarantees excellent resistance to grease, achieving the highest Kit test rating, and a significantly reduced HVTR compared to uncoated and commercial samples. Moreover, the comparison between the results obtained showed that spray coating resulted in less use of suspension and faster process, leading to the best results in terms of barrier against contaminants and grease resistance.

1 | Introduction

The competition between paper and plastic packaging to be defined as the most used solution for food packaging is ongoing, while scientific research is increasingly focused on sustainable solutions made up of materials from renewable sources that are also recyclable, biodegradable, and/or compostable [1]. About 31% of the global food packaging market in recent years is represented by paper and paperboard-based packaging [2, 3].

Nevertheless, these packaging solutions have limitations and critical issues for food items with a long shelf-life. They are

typically suitable only for packaged dry solid matter, often show poor barrier properties towards gas, water and grease and are also susceptible to microbial attack [4]. Additionally, they may be contaminated by Polyfluoroalkyl substances (PFAS), resulting from the use of printing inks or chemical mixtures use for technological purposes [5, 6]. PFAS especially contaminate recycled paper and paperboard, where their presence is due to intentional addition, i.e., chemical mixtures for conferring water and oil repellent properties, or to accidental transfer during transport, storage and disposal phases before recycling process [7, 8]. Furtherly, often exhibit problems with the migration of MOHs (mineral oils hydrocarbons) [9]. For the migration of MOAH (mineral oil aromatic hydrocarbon) and MOSH (mineral oil saturated hydrocarbon), the EU Commission proposed limits into food, respectively, 0.15 and 0.6 mg kg^{-1} of food [10]. Considering the aforementioned limitations, paper, cardboard and paperboard packaging solutions are frequently added of functional additives, provided with various chemical coatings and are often combined with synthetic materials and aluminium foil. These treatments aim not only to reduce or prevent migration but also to improve and control the technological characteristics and properties of these packaging materials. Petroleum-based polymers, commonly used for this purpose, include almost all the polyolefins (i.e., LDPE, HDPE and PP), polyethylene terephthalate (PET), ethylene vinyl alcohol (EVOH), ethylene vinyl acetate (EVA) and few others. However, the use of synthetic coatings, as the presence of extraneous components, can reduce the biodegradability of paper and board and make the recycling process more difficult and challenging [11–13].

Consequently, recent research has focused on the development of biobased coatings from biopolymers such as polysaccharides, proteins and waxes or from bioplastics such as polylactic acid (PLA), polycaprolactone (PCL) and polyhydroxy alkanoates (PHA) to improve the functionality of cellulosic packaging solutions, reduce environmental impact and preserve the easy recycling of paper and paperboard [4, 12, 13].

In recent years, the use of cellulose derivatives and the interest in nanomaterials, such as micro- and nano-fibrils or nanofibrillated cellulose (MFC/NFC), for coating applications on paper and paperboard, has been growing steadily [13–15]. The first method to produce them from wood pulp was found by Herrick et al. [16] and Turbak et al. [17]. It involved applying various cycles of high-pressure homogenization to a dilute suspension of fibers to break the hydrogen bonds and open the cellulose fibers, resulting in micro- and nano-fibrils of cellulose. Subsequent research demonstrated that pre-treating the suspension with chemical or enzymatic processes facilitates the achievement of fibrillation [18–21].

High-pressure homogenization is one of the most widely used mechanical methods for the production of cellulose microfibril and nanofibrils [22-24]. It consists of subjecting cellulose fibres to a rapid pressure drop with shear forces that promote a high degree of fibrillation. It has been shown that several homogenization steps lead to fibrils of increasingly smaller diameters [25]. MFC/NFC can also be produced through grinding [26], microfluidization [27] and refining [28]. These cellulose derivatives have been studied for their vapour and gas barrier properties, their resistance to oils and grease [29, 30] and for their ability to contrast the absorption of polar and nonpolar liquids [31, 32] According to recent research [12, 33], a relatively low coating grammage of microfibrils–nanofibrils on papers, about 10 g m^{-2}, can provide adequate water and oxygen barrier properties. This indicates the importance of the method of application of the coating to achieve the desired properties.

Generally, the application of suspensions containing micro- and nano-fibrils of cellulose to paper and paperboard is carried out through bar coating, roll coating and size press coating [34]. These methods, to be functional, fortunately require low coating weights, despite involving multiple application steps. However, coatings are often not continuous or uniform, resulting in inadequate barrier properties. Bar coating allows good control over the coating distribution, but unfortunately, it is limited to laboratory scale, as it is not considered practical for industrial use [35].

To obtain more homogeneous coatings, spray coating can be used. This method is compatible with suspensions of micro- and nanofibrils of cellulose, with the only drawback being related to the viscosity and solids content of the suspension, i.e. a low solids content and low viscosity are required. However, it allows operation at high speeds and therefore offers greater industrial scalability [34]. There are many studies in the literature evaluating the effect of the application of micro- and nano-fibrils of cellulose (MFC/NFC) on paper and paperboard packaging, with different coating processes. Mousavi et al. (2017) and (2018) used two forms of NFC, refiner NFC (rNFC) and grinder NFC (gNFC) with solid contents of approximately 1.5 wt% and 3 wt%, respectively, with and without carboxymethyl cellulose (CMC), to develop functional coatings aimed at improving barrier properties. They observed an improvement in barrier properties as a function of coat weight and surface coverage [36, 37]. Lavoine et al. (2014) studied the effect of applying a 2 wt% of MFC, obtained by microfluidization, using both bar coating and size press process. They observed a 70% reduction in air permeance and highlighted that improvement in the properties of paper and paperboard substrates depends on the substrate type and on the type and quantity of coating used [38]. The general objective of this study is to assess the effectiveness of a coating based on micro- and nano-fibrils of cellulose as a biobased, sustainable alternative to synthetic coatings. Specifically, the work aimed to optimize the coating method on the paperboard commonly used to manufacture food packages, understanding the influence of some process variables. The research compares the conventional method (bar coating) with a more innovative method (spray coating) with respect to the migration of mineral oils hydrocarbons (MOH) and grease resistance. The improvement of these key properties could extend the use of cellulose materials to applications that are currently problematic or prohibitive for paperboards and open new and profitable uses of recycled cellulose materials. To date, recycled paper and paperboard packaging are critical for the migration of contaminants from printing inks or recycling processes [39, 40]. This limits their use for food packaging applications where virgin paper is widely used. Adapting the use of functional coatings based on MFC/NFC, also to recycled paper and paperboard packaging could broaden the use without compromising food safety and further recycling.

2 | Materials and Methods

2.1 | Materials

A commercial paperboard (Control_A), largely used for dry foods packages, with 0.450 mm of thickness and 280 g m^{-2} of grammage, supplied by Commer Carta (Commer Carta srl. Locate di Triulzi, Milano, Italy), was used as a reference sample and as a substrate for the coating. A commercial paperboard for food packaging with a functional barrier provided by a synthetic but biodegradable polymeric coating (about 15% w/w) intended to protect the food against mineral oils and other undesired substances, (MM Frohnleiten GmbH, Austria), named as Control_B, was used as a second reference sample for the experimental design analyses. The aqueous suspension of micro- and nano-fibrillated cellulose (MFC/NFC) was provided by CLS Providentia (CLS Providentia SRL—Social Enterprise, Saronno, Varese, Italy). For analytical determinations, n-heptane, toluene and castor oil, with a purity > 90%, where purchased from Carlo Erba reagents (Carlo Erba, Milan, Italy).

2.2 | Chemical–Physical Characterization of Microfibrillated/Nanofibrillated Cellulose Coating Suspension

To prepare the suspension, the producer used a biomass rich in cellulose (about 51%), coming from a seed tegument widely used for food, and natural functional ingredients, a thickening and film forming agents, to stabilize its structure and maintain stability (the complete formulation and production process are protected by trade secret). To obtain extensive fibrillation, the suspension was subjected to several high-pressure (> 1000 MPa) homogenization cycles. Before the coating application, in order to have a general characterization of the suspension, the pH, dynamic viscosity, dry matter content and the ratio between micro- and nano-fibrils were measured, and dynamic light scattering (DLS) measurements, FTIR and TEM observations were also carried out. To perform the general characterization, the producer provided us with both the stabilized suspension with the functional ingredients and a suspension of raw biomass without additives.

2.2.1 | pH

The pH was measured under stirring using a CyberScan pH 310 (Thermo Fisher Scientific Inc., Waltham, MA, USA), previously calibrated with buffer solutions at pH 7.0 and 4.0 (Sigma-Aldrich, Merck KGaA, Darmstadt, Germany). Ten measures were conducted, and the result is expressed as average value ± standard deviation.

2.2.2 | Dynamic Viscosity

The dynamic viscosity was measured using a compact modular rotational rheometer, MCR302 (Anton Paar, Graz, Austria). The analysis employed a plate-plate system, with a Peltier plate of 49.978 mm in diameter. For each sample, the moving profile was set to 'Viscoelastic', and the temperature of the lower plate was maintained at 25°C. To facilitate sample positioning, the Peltier plate was initially raised to a gap of 60 mm and then lowered to an analysis distance of 1 mm. Three separate analyses were performed at different rotation speeds of the Peltier plate (20, 40 and 60 rpm), each consisting of 100 measurement points. The results are expressed as average values ± standard deviation of the last 40 points of analysis.

2.2.3 | Dry Matter

The dry matter of the suspensions was determined according to the AOAC official methods [41]. The analysis was conducted in triplicate, and the result is expressed as average ± standard deviation.

2.2.4 | Quantification of Microcellulose /Nanocellulose Fibrils Ratio

The ratio between microcellulose and nanocellulose fibrils was determined according to the method used by Schnell et al. 2018 [42], on a sample of the aqueous suspension homogenized without functional ingredients. The suspension, made up of MFC and NFC at 0.14 wt.%, was centrifuged at 2800 *g* at room temperature for 20 min. The nanofibrillation yield, expressed in %, was calculated with the following equation:

$$\text{Nano} - \text{fibrillation yield}\,(\%) = \frac{\left(P_{M|NFC} - P_{MFC}\right)}{P_{M|NFC}} * 100$$

where $P_{M|NFC}$ is the solid mass of coating suspension and P_{MFC} is the weight of the micro-fibrillated fraction corresponding to the centrifuged sediment.

2.2.5 | Particle Size Distribution

The dimensions of microfibrils and nanofibrils in MFC/NFC suspension were investigated by DLS measurements (mod. Litesizer500, Anton Paar, Graz, Austria), performed at 25.0°C ± 0.1°C with a 35-mW laser diode light ($\lambda = 658$ nm) and collecting the scattered light at 15° and 90°. Before the DLS measurements, the sample was diluted to 1:100 *w/w* with distilled water and filtered with a 0.2 μm filter. The analysis was assessed in triplicate, and the results are expressed as average values ± standard deviation.

2.2.6 | Cellulose Fibrils Morphology

Transmission electron microscopy (TEM) was used to verify the shape and size of micro- and nano-cellulose fibrils. The analysis was carried out using a Talos F200S G2 microscope (Thermo Scientific, Brno, Czech Republic), running at an acceleration voltage of 200 kV. A drop of MFC/NFC diluted solutions was pipetted onto a nickel grid (200 mesh). TEM micrographs were analysed by means of ImageJ software (v. 1.53a, National Institutes of Health, Bethesda, Maryland, MD, USA).

2.2.7 | Chemical Structure

The chemical structure of the suspension's components and their possible changes after high-pressure homogenization were investigated by Fourier-transform infrared-attenuated total reflection spectroscopy, FTIR. The FTIR spectra of freeze-dried cellulose suspension were recorded using a Vertex 70 (Bruker, Germany) spectrometer equipped with an attenuated total reflection (ATR) Golden Gate diamond. All spectra were recorded in adsorption mode in a wavenumber range of 4000–600 cm^{-1} with an accumulation of 32 scans at 4 cm^{-1}.

2.3 | Paperboard Coating Process and Characterization

2.3.1 | Coating Application Methods

Rectangular sheets of 21 × 30 cm were cut from the commercial paperboard reel (Control_A) and covered with the MFC/NFC coating suspension (~3.6% solids), using two different coating methods: BC and SC. For BC, an automatic applicator (RK, R Control Coater, URAI, Assago, Milano, Italy) was used. The coating machine was equipped with eight different meter bars (Mayer bars), with different wire diameters capable of depositing wet films from 6.35 to 101.6 μm thickness at different and controlled speeds. Three bars were used, which respectively had a wet film thickness of 38.1, 63.5 and 101.6 μm. For BC the coating step was always repeated twice to obtain the most uniform coverage, and between the two steps the paperboards were predried before applying the second layer. For the SC method, a prototype apparatus was used. A printing–cutting plotter machine was modified to drive a spray-painting system. A compressed air spray gun, with a 1.7 mm diameter nozzle was adapted to the plotter; the advancing speed and the aerosol working pressure were adjustable and controlled, by the software of the plotter and by a pressure regulator of compressor respectively. The coating suspension (~3.6% solids) was diluted with distilled water (2:1) before spray coating, and only one coating step was carried out.

2.3.2 | Design of Experiment (DOE)

To optimize the paperboard coating process, an L^F factorial design with three levels and two factors was used for each coating method on Control_A. The two experimental designs included 12 experimental conditions with four centre point replicates. As independent variables, wet film (38.1–63.5—101.6 μm) and speed of the automatic film applicator (1.5–3.25—5 m min^{-1}) were chosen for the first factorial design (BC). For the second factorial design (SC), the two independent variables chosen were: Speed (15–30–45 m min^{-1}) and Pressure (1.5–2.5–3.5 bar) of the spray coating (Table 1). After coating application, the samples were dried in an oven at 60°C for 1 h. The samples were kept for 24 h at room temperature before analyses. For each experimental condition, the coating grammage, grease resistance (kit test) and heptane vapour transmission rate (HVTR) were measured and compared to the control samples (Control_A and Control_B). On the best samples selected from both experimental designs and on uncoated paperboard, the water absorption (Cobb test), water and castor oil contact angles, the water vapour transmission rate (WVTR) were finally measured; in order to assess the performance improvements and the comparison between the two coating methods, an assessment of the paperboard surface by SEM and AFM observations was also carried out.

2.3.3 | Grammage

The grammage of each sample, uncoated and covered through BC and SC methods according to the DOE, was calculated after conditioning (105°C for 90 min) by weighing with an analytical balance (accuracy 0.0001 g). For all analyses, circular specimens (about 55 cm^2) were used and the diameters of the samples were measured with a digital calliper (Borletti, Milano, Italy). The coating grammages were calculated as the difference between the weight of the coated and uncoated paperboard and expressed as g m^{-2}. The analysis was performed eight times and the results expressed as average value ± standard deviation.

TABLE 1 | Variable experimental design with samples coding.

Bar coating factorial design			Spray coating factorial design		
Variable		Sample code	Variable		Sample code
Wet film thickness (μm)	Speed (m min^{-1})		Speed (m min^{-1})	Pressure (bar)	
101.6	5	B101-5	45	3.5	S45-3.5
101.6	3.25	B101-3.25	45	2.5	S45-2.5
101.6	1.5	B101-1.5	45	1.5	S45-1.5
63.5	5	B63-5	30	3.5	S30-3.5
63.5	3.25	B63-3.25	30	2.5	S30-2.5
63.5	1.5	B63-1.5	30	1.5	S30-1.5
38.1	5	B38-5	15	3.5	S15-3.5
38.1	3.25	B38-3.25	15	2.5	S15-2.5
38.1	1.5	B38-1.5	15	1.5	S15-1.5

2.3.4 | Grease Resistance

The grease resistance was tested following the Kit 12 test [43]. This test involves the preparation of 12 solutions with varying proportions of castor oil, heptane, and toluene. The lipophilic strength of the solution increases from 'solution 1' (least lipophilic) to 'solution 12' (most lipophilic). A drop of each solution was gently released onto the surface of the sample; after 15 s, it was quickly removed with a clean absorbent cloth, and the test area was immediately examined. A failure in the test was denoted by a darkening spot in the test area due to the diffusion of the solution. The test was passed when, after the removal of the drop, no solvent stains were observed. The tested sample was given the number of the solution that passed the test as the result. The results obtained have been expressed as average value ± standard deviations.

2.3.5 | HVTR

The HVTR was measured through the gravimetric method described by Gaudreault et al. 2013 [44] with modifications. Circular paperboard disks 8.65 cm in diameter, coated and uncoated, were cut and placed on aluminium cups of the same diameter. Before sealing, a cotton pad soaked in 9 mL of heptane was placed in the cups. To guarantee better sealing, the paperboards were closed with a plastic gasket in polytetrafluoroethylene (PTFE), with two aluminium square flanges screwed to the four corners with screws and bolts. The hermeticity of the system was tested by assessing the transmission of heptane vapour through uncoated paperboards covered with a 50-μm-thick adhesive aluminium foil. The samples were stored at 30°C and weighed every 30 min. The transmission rate of heptane through the exposed surface of paperboard was determined by plotting the weight gain as a function of time for the period of linear weight increase ($R^2 > 0.99$) and was calculated as follows:

$$HVTR = \frac{\Delta W}{\Delta t} \cdot \frac{1}{A}$$

where $\frac{\Delta W}{\Delta t}$ is the slope of the linear regression of the weight increase of the cups as a function of time ($g\,h^{-1}$) and A is the surface area of the exposed film ($5.81 \cdot 10^{-3}\,m^2$). The results have been expressed as average value ± standard deviations ($g\,h^{-1}\,m^{-2}$).

2.4 | Characterization of Best Performing Coated Paperboard

2.4.1 | Water Uptake

The water uptake is a measure of the amount of water absorbed by the surface of paper and paperboard, in a given time. This property was evaluated using the $Cobb_{300}$ test, in accordance with the official method T441 om-9 [45], where water uptake is measured after 300 s of contact with water. The Cobb value represents the amount of water absorbed per unit area ($g\,m^{-2}$) and was measured according to the following equation:

$$Cobb_{300} = (W_{300} - W_0) \times 100$$

where W_0 is the weight before contact with water, while W_{300} is the weight after contact with water. All the best samples were tested two times, and the results have been expressed as average value ± standard deviation.

2.4.2 | WVTR

The WVTR was determined according to the standard method ASTM E96 [46] with some modifications. Glass vials with a 10-mm internal diameter and 55-mm depth were filled with 2 g of anhydrous $CaCl_2$ (0% RH). Samples were then sealed on top of the vials with a PTFE gasket and an Aluminium crimp seal, which were placed in a desiccator containing $BaCl_2$ saturated solution (90% RH) and stored at 38°C. The WVTR was determined by plotting the weight gain of the vials as a function of time for the period of linear ($R^2 > 0.94$) weight increase (up to 4 days) and was calculated as follows:

$$WVTR = \frac{\Delta W}{\Delta t} \bullet \frac{1}{A}$$

where $\frac{\Delta W}{\Delta t}$ is the slope of the linear regression of the weight increase of the cups as a function of time ($g\,day^{-1}$) and A is the surface area of the exposed film ($7.85 \bullet 10^{-5}\,m^2$). The results have been expressed as average value ± standard deviations ($g\,h^{-1}\,m^{-2}$).

2.4.3 | CA Determinations

The surface's hydrophobicity and oleophobicity of the samples were evaluated by determining the CA values. The analyses were conducted with an OCA 15EC CA meter and OCA 20 software (DataPhysics Instruments, Germany), using the sessile drop method, at room temperature (21°C ± 1°C).

Paperboard strips of 1 × 10 cm were positioned on a film holder and, with a micro-syringe, 7 μL of water or vegetable oil (castor oil) was deposited on the paperboard surface. The water and castor oil CAs were measured immediately after the drop position (t_0) and for the castor oil also after 30 s of depositing.

For the CAs measurements of each sample, 20 replicates were considered, and the results have been expressed as average values ± standard deviation.

2.4.4 | Roughness

The Atomic force microscopy (AFM) was performed on the reference substrate (Control_A) and on the coated samples to investigate the surface roughness of the samples after coating application to indicate the best coating method. The topographic analysis was performed with the Atomic Force Microscope AUTOPROBE CP (Veeco, Sunnyvale, CA, USA) at room temperature in *noncontact mode* on a sample area of 20 × 20 μm^2. The AFM images were obtained using ProScan Data Acquisition Software, after correction of the background, and show the changes of sample surface due to coating application. For each paperboard, four observations were taken in different points,

and the results of Ave (Average) roughness have been expressed as average value ± standard deviations. The Ave roughness is given by the average deviation of the data from the average of the data (ProScan Data Acquisition Software reference manual).

2.4.5 | Surface Structure

Scanning electron microscopy (SEM) was used to investigate the distribution of MFC/NFC on the surface of paperboard. To perform SEM observation, paperboard samples were cut ($1 \times 1\,cm^2$), coated with a thin layer of gold (Au) and mounted on a stainless-steel stub with double-sided tape. A field emission Nova NanoSEM 450 (FEI Company-Bruker, Germany) at 1000x and 5000x of magnification operating at 10 kV in high vacuum conditions was used to carry out the observations.

2.5 | Data Analysis

Statistical analysis of all the results was conducted using one-way analysis of variance (ANOVA). Significant differences among groups ($p < 0.05$) were assessed by Tukey's HSD post hoc test. The choice of the optimal conditions was carried out through the creation of response surface and through the use of a mathematical function, the desirability index (DI). The DI is used to reach the best value of trade-off to determine the best response. To obtain this value, individual desirability models are created for the response of the experimental design by setting optimization criteria [47]. Specifically, a grammage value in a range of 1–15 g m^{-2} was set, a maximum HVTR value of 3.5 g h^{-1} m^{-2} with a minimum test kit value of 10. All analyses explained in this section were carried out using RStudio (version 2022.12.0 + 353; RStudio, Boston, MA). Unless otherwise stated, the experiments were performed in triplicate, and the results have been expressed as average value ± standard deviation.

3 | Results and Discussion

3.1 | Chemical–Physical Characterization of Coating Suspension

Table 2 reports the general characterization of the coating suspension with special regards for pH, FTIR spectra, dry matter, dynamic viscosity, ratio between micro- and nano-cellulose fibrils, TEM observations and DLS. As it can be inferred, the pH of the MFC/NFC suspension is close to neutral and very similar to the pH value of the dispersion in water of all the ingredients, assessed before high-pressure homogenization. This is a positive indication that the physical fragmentation method used did not significantly change the chemistry of the original cellulose and any natural functional additives used. This assumption is also confirmed by the FTIR analysis carried out on the homogenized and nonhomogenized freeze-dried suspensions (Figure S1). The FTIR spectrum shows a large band at 3281.2 cm^{-1} corresponding to the –OH stretching vibrations of CH2–OH on cellulose and bound water, indicating the formation of hydrogen bonds due to the interaction with water [48]; a small band at 2924.7 cm^{-1} corresponding to C–H stretching vibrations of cellulose [49]; and the peaks at 1408.1, 1148.6 and 1031.4 cm^{-1} corresponding to C–H oscillating vibrations of cellulose, C–O–C asymmetric stretching and C–O stretching, respectively [50]. Looking carefully at the two spectra, we can see that no relevant changes have occurred in terms of amplitude or position of the peaks due to the high-pressure homogenization treatment. As shown by the dry matter value in Table 2, the suspension is very diluted (3.6% d.m.), and this low concentration of solids is most likely ideal to obtain the right fibrillation of the cellulose during the high-pressure homogenization process, limiting the energy cost of the process which is always rather high [51]. Despite this low concentration, the dynamic viscosity of the suspension appears quite high, ranging from approximately 488 to 1213 cP, depending on the rotation speed of the viscometer. The exponential reduction in viscosity, as a function of rotation speed, is indicative of a viscoelastic behaviour of the suspension, related to the aspect ratio of the nanofibrils and their flexibility [52].

TABLE 2 | General characterization of MFC/NFC coating suspension.

Test	MFC/NFC coating suspension
pH	6.91 ± 0.04
Dynamic viscosity 20 rpm (cP)	1212.90 ± 20.34
Dynamic viscosity 40 rpm (cP)	673.28 ± 5.05
Dynamic viscosity 60 rpm (cP)	487.62 ± 1.53
Dry matter (%)	3.60 ± 0.17
MFC (%)	85.99 ± 3.04
NFC (%)	14.01 ± 3.04
DLS—hydrodynamic diameter (nm)	153.68 ± 25.26
DLS—polydispersity index (PDI %)	25.83 ± 1.38
Aspect ratio from TEM observations	104.51 ± 16.85

The TEM observations (Figures 1) confirm the extensive fibrillation of the cellulose fibre bundles and the fragmentation of the fibres present in the raw biomass, where, as observed by the optical microscope (Figure S2), the bundles length was around 50 μm. High-pressure homogenization allowed a notable reduction in the length of the fibrils but with a highly variable distribution (range 1.2–11.7 μm). TEM observations also confirm that diameter reduction, rather than full-length shortening, is the predominant mechanism of cellulose fibrillation; in fact, the diameter measurements are in nanometres scale (range 16–95 nm). This leads to an aspect ratio value just below 100. The higher the aspect ratio, the higher the viscoelastic behaviour, and this obviously greatly affects the coating process and the homogeneity of the coating.

Furthermore, the apparent flexibility of the nanofibrils (see Figure 1) prefigures an extensive possibility of mutual entanglement, which can lead to the formation of a compact MFC/NFC layer during the cardboard coating process.

The microscopic observations of the fragmented cellulose fibres revealed a heterogeneous morphology, showing both micro and nano fibrils. The gravimetric method, used to quantify the ratio

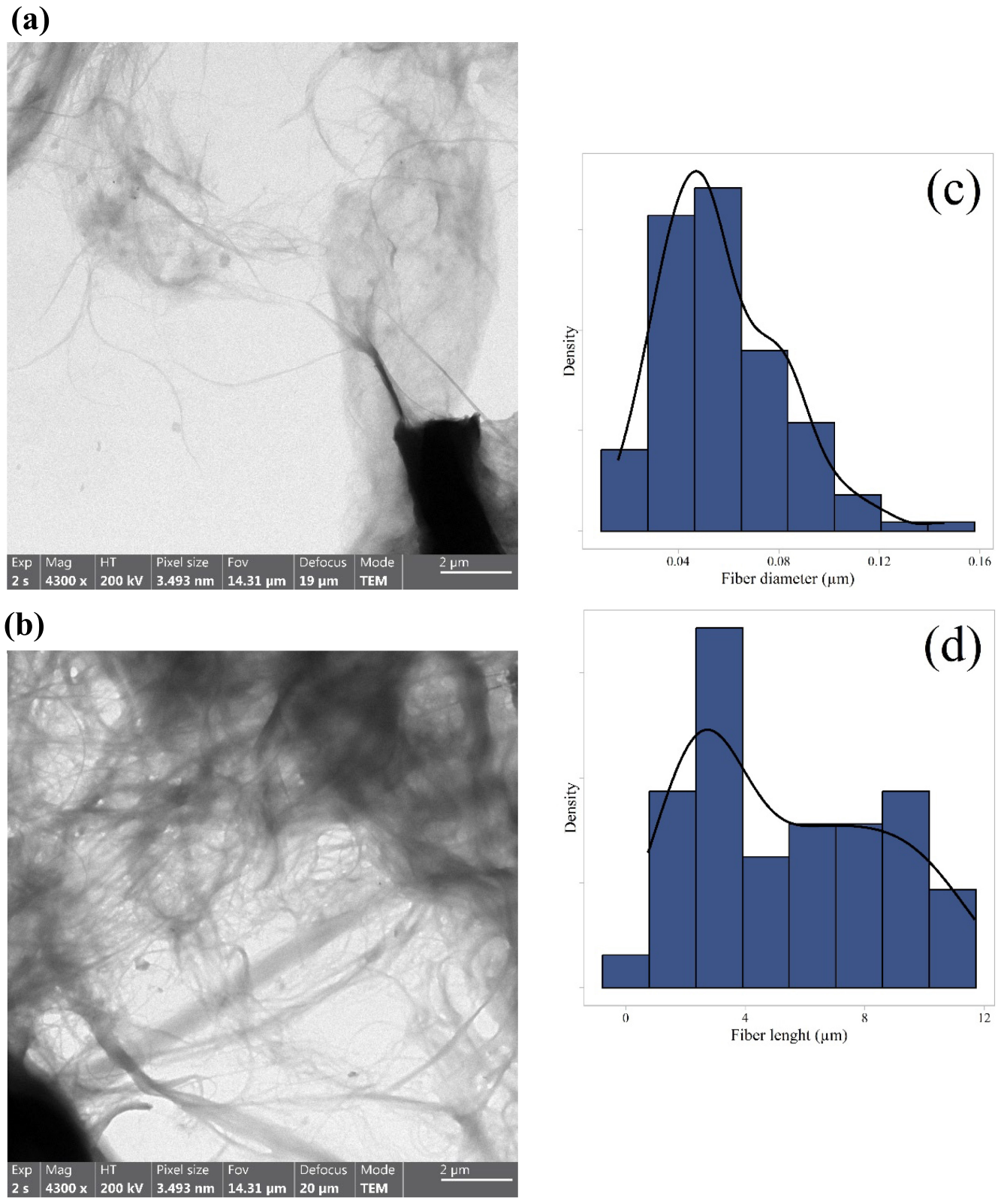

FIGURE 1 | Transmission electron microscopy, TEM, images of the microfibrils and nanofibrils cellulose suspension at 4300×magnitude. (a) Fibrillation of the microscopic cellulose fibre. (b) Entanglement network of microcellulose–nanocellulose fibrils. The insets show the fibre diameter distribution (c) and the fibre length distribution (d) of the cellulose suspension subjected to high-pressure homogenization and consequent microfibrillation–nanofibrillation.

of micro/nano cellulose fibrils, gave an average value of 86% micro fibrils (see Table 2), though with a high deviation due to the presence of particles of different sizes. This is also confirmed by DLS measurements and in particular by the polydispersity index (PDI) higher than 25%. The PDI is a measure of the width of particle size distribution. Values below or equal to 10%

indicate that the sample is monodisperse [53], while a higher PDI suggests that the morphology and distributions are more complex as in this case [54].

The fact that the MFC/NFC are not spherical poses some problems on the sizes estimated by DLS, which analyses the data in spherical approximation, mathematically treating the particles as spheres moving with Brownian motion. Differently from spheres, the hydrodynamic stresses will depend on the orientation of the fibrils, determining an anisotropic motion of the scatterer [55]. Consequently, fibrils are possibly detected by DLS as equivalent Brownian spheres with a smaller average size [56]. The presence of a high percentage of nanofibrils, in principle, should allow a more homogeneous and continuous coverage of the paperboard surface during the coating process and, consequently, higher performances of the coated paperboards.

3.2 | Paperboard Coating Process and Characterization

3.2.1 | Coating Grammage

Once the coating has been applied with the two methods (2.3.1), according to the experimental design (2.3.2), the coating grammages of all samples of the two-factorial design were measured, and the results are reported in Table 3. Using the BC method, the grammages were in the range of 2.36 ± 0.82 and $14.75 \pm 0.68\,g\,m^{-2}$; while using the SC method, the grammages were in the range of 1.55 ± 0.52 and $8.85 \pm 3.05\,g\,m^{-2}$. Overall, the minimum grammages are very similar, while the maximum ones show a significant difference, with the SC method having spread smaller amount of coating, in rather shorter times. For both coating methods, of course, the highest coating weights were achieved with lower coating speeds, higher wet films deposited by the bars or higher spray system pressure, but it seems relevant to note that the SC allows similar grammages at 10 times higher speeds and in a single step, with a more diluted suspension. Using a more diluted suspension we were certainly able to obtain a more homogeneous coating, but this implied a longer drying process because the quantity of water to evaporate was greater. For the BC conditions, an amount of water in the range 63–110 g m^{-2} was evaporated, for the best SC conditions it was necessary to evaporate a quantity of water in the range 481–678 g m^{-2}. It is also worth noting that the increase in the total grammage of coated paperboard was very low, below 3% compared to the grammage of uncoated samples.

3.2.2 | Grease Resistance

The grease resistance was determined for all experimental conditions of the two-factorial design using the Kit test (2.3.4) to assess the minimum amount of coating providing samples with sufficient barrier to pass the test and to select the best-performing coating conditions. Above a Kit number of 8, a cellulosic material is generally considered grease-resistant [35, 57] and suitable for food packaging use. All the experimental samples were compared with both the uncoated base sample (Control_A) and the sample covered with synthetic polymer (Control_B), both showing scarce resistance to grease (Table 3).

As for bar-coated samples, all of them demonstrated excellent grease resistance, according to the maximum Kit Test value (Table 3).

Most of the spray-coated samples also demonstrated excellent grease barrier, reaching the value of 12. However, three samples (namely, S45-1.5, S30-1.5 and S151.5) did not reach the minimum acceptability threshold for use as food packaging (Table 3). These cartons were sprayed at the lowest pressure tested (1.5 bar), which proved insufficient to ensure uniform coverage, most likely due to an atomization defect. Atomization, in the context of whatever SC method, refers to the process of breaking up the liquid coating into fine droplets to create the aerosol. The aerosol pressure is a critical factor that influences the efficiency and effectiveness of the final coating application, and more viscous suspension may require higher pressure to atomize effectively [58, 59].

A similar behaviour was observed in the literature: Aulin et al. 2010 [60] assessed the time of castor oil penetration and observed that grease resistance was improved by the addition of a cellulose suspension on base paper. Hassan et al. 2016 [61] also noted an improvement in grease resistance after coating paper sheets with micro- and nano-fibrillated cellulose (MFC or NFC). Furthermore, Lavoine et al. 2014 [57] and Zhang et al. 2021 [62] evaluated grease resistance using the Kit value, and both observed that when paper was coated with MFC or other cellulose-based suspensions, the grease resistance was enhanced. Given the excellent grease resistance achieved with the experimental samples, future developments could consider the effects of folding on the Kit test value to assess the performance retention of the coating in practical applications [63].

3.2.3 | HVTR

To evaluate the resistance to potential MOH migration, the HVTR was measured for all samples in both experimental designs, as well as for the two control samples. Tiggelman et al. (2012) [64] proposed heptane vapour as a good simulant for MOH and suggested HVTR to assess the diffusion performance of MOH through packaging materials, since the vapour pressure at room temperature of the MOH alkanes (composed of large alkanes, range *C24–C16*) is far below the vapour pressure of smaller alkanes like heptane and hexane. The gravimetric method for HVTR has been widely used since then [44, 65, 66]. Generally, a value of HVTR below $0.42\,g\,h^{-1}\,m^{-2}$ is considered a good mineral oil barrier, while if the value exceeds $20.83\,g\,h^{-1}\,m^{-2}$, the barrier is ineffective [44]. The results for HVTR (Table 3) suggest that the MFC/NFC coating significantly improved the barrier against heptane and mineral oil hydrocarbons, given the 95.3%–99.3% HVTR reduction compared to the uncoated sample (Control_A). Previous studies on micro–nanocellulose coatings [67] and on starch-based coatings [65, 68] demonstrated the effectiveness of such coatings on the reduction of HVTR and consequently of MOH transmission. It is worth noting that, except for the results obtained with the lowest wet film (38.1 μm), all the bar coating conditions produced similar results highlighting relatively low transmission values. Even for spray coating conditions,

TABLE 3 | Results for grease resistance (Kit test), grammage and mineral oils hydrocarbons diffusion (HVTR) for the samples of factorial designs compared to the uncoated paperboard (Control_A) and a commercial control paperboard coated with synthetic polymer (Control_B).

Sample	Kit value	Coating grammage g m^{-2}	HVTR g h^{-1} m^{-2}	Desirability index
Control_A	0	0	81.49 ± 1.74 ^{a}	
Control_B	0	42**	4.71 ± 0.58 ^{b}	
Bar coating factorial design				
B101-5	12.00 ± 0.00 ^{a}	7.43 ± 0.93 ^{c}	0.55 ± 0.22 ^{d}	0.543
B101-3.25	12.00 ± 0.00 ^{a}	10.29 ± 1.16 ^{b}	0.69 ± 0.26 ^{d}	0.493
B101-1.5	12.00 ± 0.00 ^{a}	14.75 ± 0.68 ^{a}	0.73 ± 0.21 ^{d}	0.430
B63-5	12.00 ± 0.00 ^{a}	4.13 ± 0.68 ^{ef}	1.01 ± 0.13 ^{d}	0.660
B63-3.25	12.00 ± 0.00 ^{a}	4.98 ± 0.57 ^{de}	1.40 ± 0.61 ^{d}	0.597
*B63-3.25	12.00 ± 0.00 ^{a}	5.62 ± 0.94 ^{d}	1.05 ± 0.01 ^{d}	0.597
*B63-3.25	12.00 ± 0.00 ^{a}	6.10 ± 1.09 ^{cd}	1.64 ± 0.76 ^{d}	0.597
*B63-3.25	12.00 ± 0.00 ^{a}	5.47 ± 0.77 ^{de}	1.60 ± 0.61^{d}	0.597
B63-1.5	11.70 ± 0.48 ^{a}	9.81 ± 1.34 ^{b}	1.40 ± 0.62^{d}	0.500
B38-5	12.00 ± 0.00 ^{a}	2.36 ± 0.82 ^{g}	2.23 ± 0.02 ^{cd}	0.806
B38-3.25	11.86 ± 0.38 ^{a}	2.72 ± 0.46 ^{fg}	2.23 ± 0.01 ^{cd}	0.765
B38-1.5	11.90 ± 0.32 ^{a}	5.35 ± 0.69 ^{de}	3.51 ± 0.62 ^{bc}	0.600
Spray Coating Factorial Design				
S45-3.5	12.00 ± 0.00 ^{a}	5.85 ± 1.70 ^{c}	3.87 ± 1.22 ^{c}	0.643
S45-2.5	12.00 ± 0.00 ^{a}	1.55 ± 0.52 ^{d}	3.87 ± 1.61 ^{c}	0.00
S45-1.5	2.33 ± 0.71 ^{c}	1.85 ± 0.51 ^{d}	53.93 ± 8.46 ^{b}	0.00
S30-3.5	12.00 ± 0.00 ^{a}	7.57 ± 0.94^{abc}	1.06 ± 0.00 ^{c}	0.00
S30-2.5	12.00 ± 0.00 ^{a}	6.25 ± 0.55^{bc}	1.76 ± 0.61 ^{c}	0.560
*S30-2.5	11.88 ± 0.35 ^{a}	7.77 ± 0.96^{abc}	0.99 ± 0.12 ^{c}	0.560
*S30-2.5	12.00 ± 0.00 ^{a}	8.41 ± 0.50 ^{ab}	0.95 ± 0.18 ^{c}	0.560
*S30-2.5	12.00 ± 0.00 ^{a}	5.87 ± 1.87 ^{c}	1.40 ± 0.61 ^{c}	0.560
S30-1.5	2.78 ± 0.83 ^{c}	2.73 ± 0.81 ^{d}	56.75 ± 4.4 ^{b}	0.000
S15-3.5	12.00 ± 0.00 ^{a}	8.85 ± 3.05 ^{a}	0.77 ± 0.27 ^{c}	0.502
S15-2.5	12.00 ± 0.00 ^{a}	8.24 ± 1.38^{abc}	0.85 ± 0.21 ^{c}	0.564
S15-1.5	7.13 ± 0.83 ^{b}	2.90 ± 1.56 ^{d}	8.46 ± 1.05 ^{c}	0.000

Note: Values of desirability index (range 0–1) to assess best conditions. Table entries with * are replicates in the center point of factorial design. Different letters (^{a,b,c}) on the same column indicate differences for $p < 0.05$. The value with ** is calculated based on the information in the technical data sheet.

the results were similar, with 10 out of 12 samples showing values assessed as not significantly different by ANOVA. The only significantly higher HVTR values correspond to the lowest aerosol pressure combined with high speed (S45-1.5; S30-1.5) which do not guarantee sufficient continuity of coverage, as already discussed for grease resistance (par. 3.2.2). Furthermore, the experimental samples (except the two samples above mentioned) showed HVTR values lower than the Control_B (Table 3), specifically treated with synthetic polymer to improve resistance to mineral oils but with a coating grammage five times heavier.

3.2.4 | Coating Optimization Through Factorial Designs

To determine within the factorial designs the best combinations of the two independent variables for both coating methods (BC and SC), the responses for grammage, HVTR and Kit value, individually and in combination, have been evaluated. A dual approach was used: response surface analysis and a mathematical function, aimed at identifying optimal conditions, to minimize the HVTR value while maintaining low weight and a high Kit value. In the first approach, the response

surfaces for all three responses were compared as shown in Figure 2a–c and Figure 2d–f, for bar coating and spray coating, respectively. The effects of the two independent variables investigated (speed and wet film for BC; speed and pressure for SC) are rather clear. They show, for instance, that the highest values of aerosol pressure in SC can guarantee high values of the kit test and quite low value of HVTR at all the coating speeds tested, even though a large variation in grammage occurs; while at the lowest pressure values, the effects of the coating speed are relevant, particularly for HVTR which increases sharply together with the velocity. Similarly, in BC, the highest wet films guarantee low HVTR and high resistance to fats both at high and low coating speeds but, at the lowest wet film values, the effect of the coating speed is opposite to that of SC. The second approach involves using the desirability function [47] to assess and optimize multiple variables to find the best conditions for the chosen parameters. This function returns a value, the desirability index (DI), ranging from 0 to 1 and all DIs are reported in Table 3. Results with a desirability index close to 1 are identified as the best conditions.

For bar coating method, based on an evaluation of response surfaces (Figure 2) and the DI (Table 2), two of the 12 experimental conditions tested were selected, as they optimized the chosen parameters. The selected samples were ***B38-5*** and ***B63-5***, which have 0.806 and 0.660 DI, respectively. The sample **B38-3.25**, which has the second highest value of this index, was not selected because it has equal parameters to the sample **B38-5** with a lower kit value. Also, two of the 12 experimental conditions tested were selected for SC method based on a response surfaces evaluation (Figure 2) and desirability index (Table 3). The selected conditions were **S45-3.5** and **S15-2.5**, which have 0.642 and 0.564 DI, respectively.

The samples selected from both experimental designs as the best conditions, together with uncoated paperboard as a reference, were subjected to the evaluation of water absorption test (Cobb300), water and castor oil CAs and WVTR; all these results are reported in Table 4. Finally, a surface structural analysis of the paperboard samples coated with the two methods was carried out by SEM and AFM.

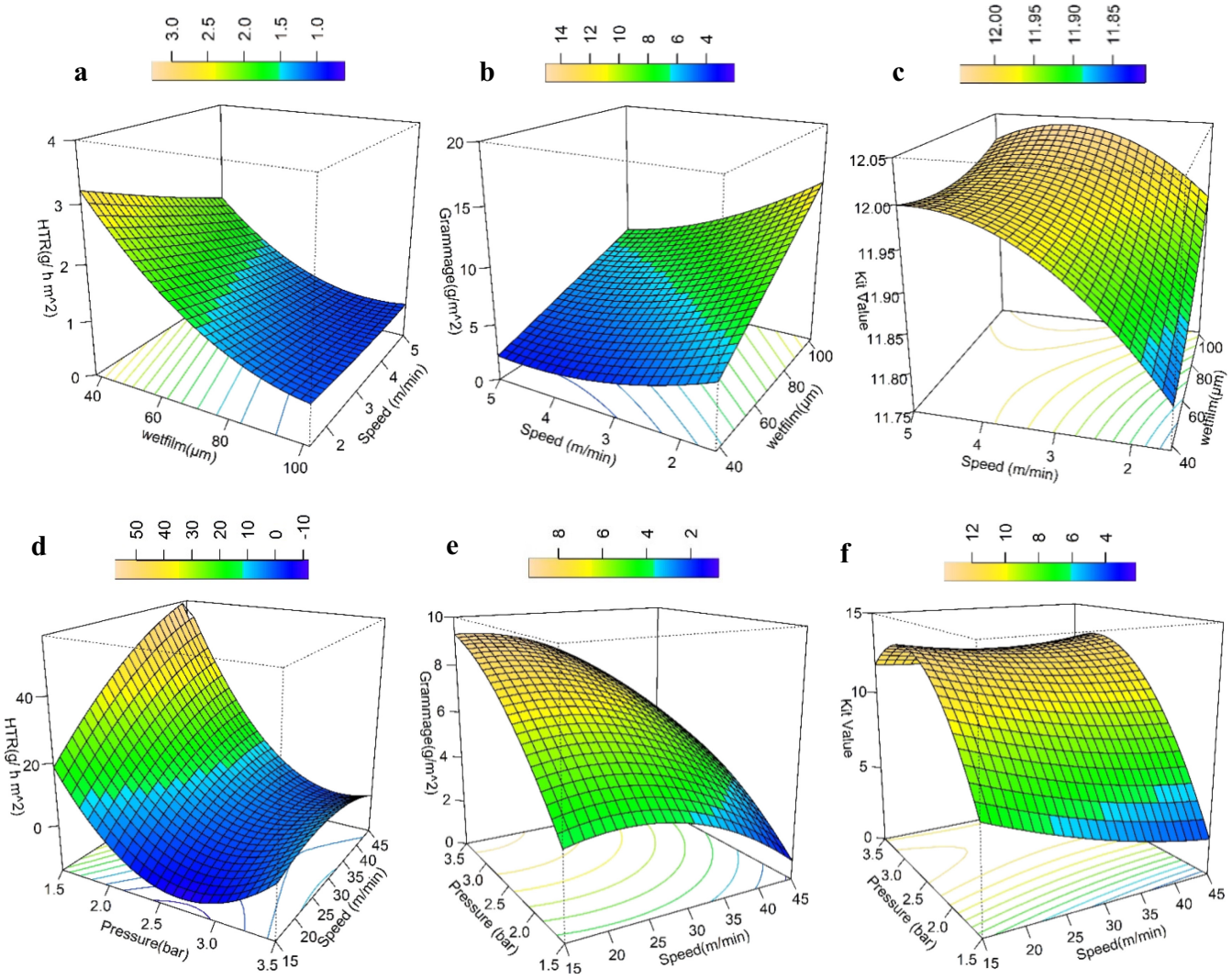

FIGURE 2 | Surface plot factorial designs. (a) HVTR ($g\,h^{-1}\,m^{-2}$) versus wet film and coating speeds (BC). (b) Grammage ($g\,m^{-2}$) versus wet film and coating speeds (BC). (c) Kit test value versus wet film and coating speeds (BC). (d) HVTR ($g\,h^{-1}\,m^{-2}$) versus aerosol pressure and coating speed (SC). (e) Grammage ($g\,m^{-2}$) versus aerosol pressure and coating speed (SC). (f) Kit test value versus aerosol pressure and coating speed (SC).

TABLE 4 | Results of water vapor transmission rate (WVTR), Cobb test 300, water and castor oil contact angles and roughness.

Sample	$Cobb_{300}$ g m^{-2}	Water CA (°)	Castor oil CA t0 (°)	Castor oil CA t30s (°)	WVTR g m^{-2} h^{-1}	Roughness (nm)
Control_A	80.03 ± 11.90[b]	103.94 ± 3.79 [a]	69.11 ± 5.00 [b]	24.57 ± 3.73 [c]	81.52 ± 5.17 [ab]	191.8 ± 3.2 [b]
B63-5	69.94 ± 0.62 [b]	90.06 ± 8.82 [b]	75.42 ± 3.23 [a]	35.36 ± 4.08 [b]	78.47 ± 6.89 [ab]	259.3 ± 3.0 [a]
B38-5	59.45 ± 0.38 [b]	91.37 ± 4.60 [b]	71.21 ± 0.95 [ab]	35.18 ± 4.82 [b]	84.07 ± 3.82 [a]	216.0 ± 13.0 [b]
S45-3.5	76.24 ± 7.25 [b]	94.60 ± 6.00 [b]	75.31 ± 4.07[a]	43.43 ± 4.03 [a]	68.53 ± 4.17 [c]	116.8 ± 1.2 [d]
S15-2.5	106.23 ± 1.6 [a]	92.76 ± 4.92 [b]	74.16 ± 4.94 [a]	44.78 ± 4.08 [a]	74.65 ± 2.31 [bc]	142.4 ± 1.41 [c]

Note: Different letters in the same column indicate significant differences for $p < 0.05$.

3.3 | Characterization of Best Performing Coated Paperboard

3.3.1 | Water Uptake

Adding MFC-NFC coating does not improve the water absorption property. On the contrary, the greater the amount of coating applied, the greater the increase in water absorption values. The paperboard coated with the spray method (***S15-2.5***), which has the highest grammage, also has the highest value of water absorption. This is likely linked to the high hydrophilicity and the large specific surface area of the micro and nano cellulosic fibres. In addition, it is also associated with the nature of the paper material used, which is very porous and with water absorbing capacity. Similar results were found by Lavoine et al. (2014), in their study on MFC, which reported that the addition of MFC increased the water absorption capacity, according to the high affinity of the coating towards water [57].

3.3.2 | CA Value

The contact angle (CA) value of the samples is useful and important for characterizing the material surface, assessing the effect of coating application and indicating the hydrophilic, hydrophobic, oleophilic or oleophobic nature of the paperboard sample (Figure S3). A lower water CA indicates the hydrophilic nature of the material, while a value > 90° indicates poor wettability and a hydrophobic nature [69, 70]. Table 4 shows the values of water CA and castor oil CA at the time of deposition (*t0*) and after 30 s (*t30*). As regards the water CA, it is worth emphasizing, as a preliminary point, the high value of the water CA of the uncoated paperboard (Control_A) which makes it appear to be a hydrophobic surface. The water CA reduction after the coating, for all the samples selected as the best conditions, is not surprising for the nature of the coating and the increased homogeneity of the surface. No statistically significant differences exist between BC and SC methods, and even though the application of the suspension of micro–nano cellulose fibrils resulted in a decrease in the CA values, the materials remain hydrophobic because the angle is always > 90°.

For castor oil CA, at *t0* of deposition, the measured values are significantly different from the control (Control_A), except for the BC sample ***B38-5*** that shows a value more similar to the control sample. This effect is likely due to a more homogeneous distribution of the micro– nano-fibrils suspension obtained with the spray coating coverage and due to the higher grammage of other experimental sample, which creates a more stable and less interactive surface against castor oil.

Instead, CA values of coated samples after 30 s from the drop deposition (CA t30s) are significantly ($p < 0.05$) higher than those of the control paperboard. This result is fully in line with the better grease resistance of the coated samples compared to the control sample. It is worth remembering that passing the Kit 12 test means showing repellency to lipophilic substances for 15 s. Furthermore, the samples coated with spray coating show statistically higher value ($p < 0.05$) than the samples coated with bar coating, indicating a better distribution of the suspension on the surface.

According to the Wenzel model, when the water CA $\theta < 90°$, an increase in surface roughness enhances the hydrophilic character of the material, increasing its wettability. Conversely, for hydrophobic surfaces $\theta > 90°$, increased roughness further accentuates the hydrophobic nature, reducing the wettability [71]. The relationships between AFM analysis and water CAs measurements demonstrate consistency with the Wenzel model, indicating that surface roughness amplifies the material's native wettability. In samples coated using BC technology, the rougher surface may lead to localized material accumulation, introducing heterogeneities that promote localized wetting while still maintaining minimal hydrophobicity ($CA \geq 90°$). In contrast, spray-coated samples exhibit a more homogeneous and uniform distribution of the micro- and nano-fibril suspension. This smoother morphology results in reduced localized wetting and a slightly lower CA, still within the hydrophobic regime ($CA > 92°$). This suggests that spray-coated surfaces may have a more stable and controlled interaction with water due to the uniformity of the coating, despite the minor reduction in CA.

3.3.3 | WVTR

The WVTR results for coated and uncoated paperboards (Table 4) show a little improvement in water vapour resistance due to the application of the MFC/NFC coating suspension by the SC method, probably due to its better coverage homogeneity than the BC method, whose results are not significantly different ($p > 0.05$) from the control sample. In the case of the spray-coated samples, the WVTR decreased by 8.43%–16%. Similar results were presented by Zhang et al. 2021 [72], in their study on microfibrillated cellulose. The reduction in WVTR, however, is of little relevance for these kinds of packaging materials which are mainly addressed to manufacturing paperboard boxes for dry pasta and not sealed package boxes; the test was performed only to investigate the continuity of the coating coverage in the two compared coating technologies, using a different approach.

3.3.4 | Surface Structure

SEM was used to investigate the surface of the coated samples and compare it with the Control_A paperboard. Figure 3 shows the SEM images of uncoated (a) and coated (b–e) paperboard, selected as best conditions, at 1000× magnitude with a section highlighted at 5000× magnitude. In uncoated paperboard, the fibres are clearly visible, as are the spaces between the crossed fibres. These are responsible for the poor resistance to water and oil. The structure with gaps and crisscrossed fibres is typical of paper and paperboard material [57, 73, 74]. In the images of coated paperboard (b-e), the sample surface is entirely covered by micro and nanofibrillated cellulose, and no more pores were noticed; similar results were achieved by Lavoine et. al. 2015 [74] in their study on MFC-coated paperboard. Furthermore, in the images of coated paperboards, it is possible to observe the

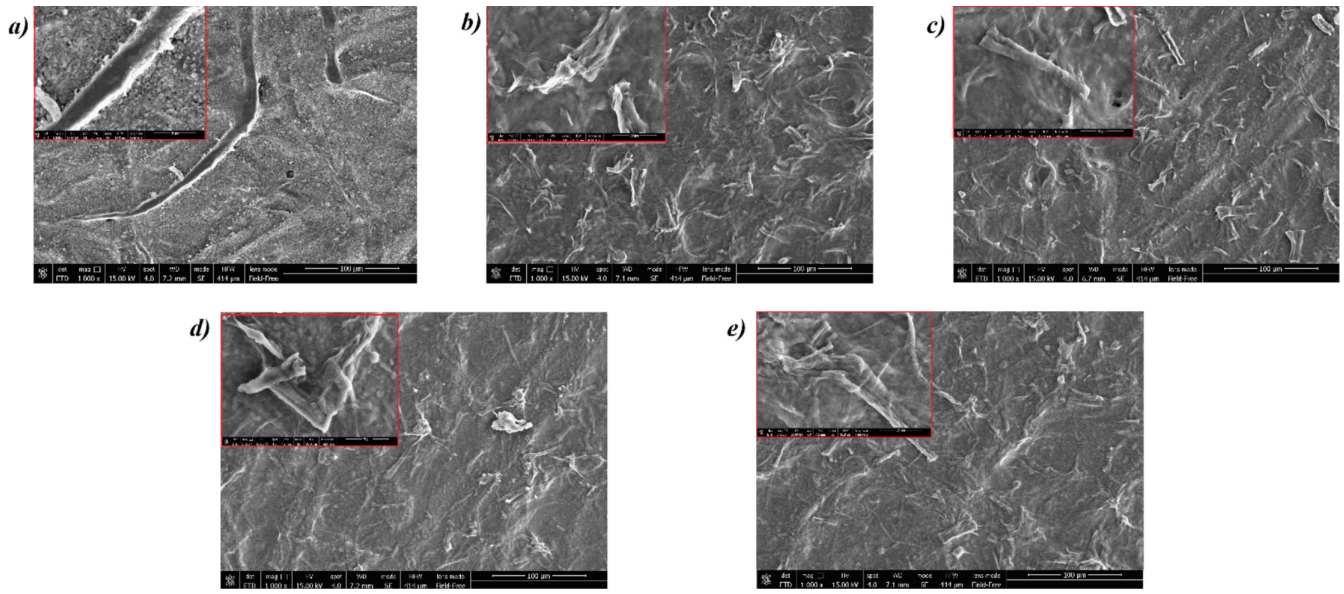

FIGURE 3 | SEM image of (a) Control_A (uncoated) sample; (b, c) best conditions of bar coating factorial design *B6_v = 5, B4_v = 5*; (d, e) best conditions of spray coating factorial design *V45_p = 3.5*, *V15_p = 2.5*.

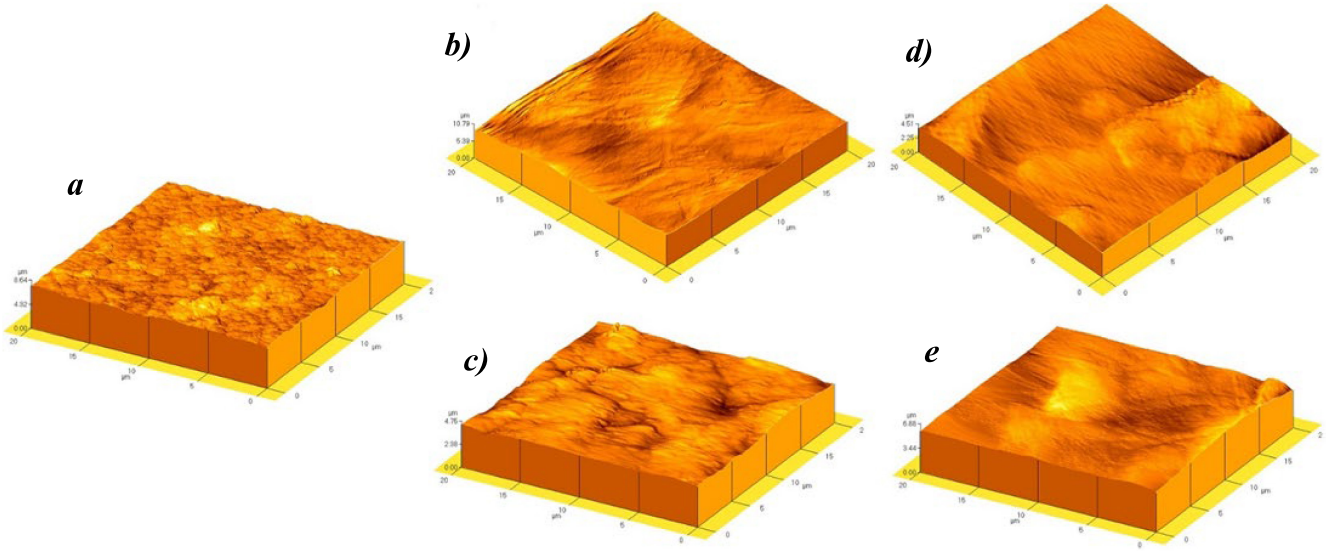

FIGURE 4 | 3D Topography, AFM images of (a) Control_A (uncoated) sample; (b, c) best conditions of bar coating factorial design B63-5, B38-5; (d, e) best conditions of spray coating factorial design S45-3.5, S15-2.5.

structure of fibrils and some pieces of fibrils, broken or with reduced dimensions, due to the fibrillation process. The image also clearly shows that the sprayed samples (d,e) have a more homogeneous surface due to more continuous coverage, as also detected by the AFM results.

To investigate the homogeneity and the roughness of the surface, AFM was used. Figure 4 shows the 3D topographies of paperboard samples analysed, while the roughness values in *nm* are reported in Table 4.

The surface appearance of Control_A is clearly distinguishable from all the others, showing a regular presence of small craters and denoting a roughness level comparable to the bar-coated samples. This is the consequence of the industrial production of the control paperboard, obviously very different from the laboratory-scale production of the bar-coated samples. The bar-coated samples (4b,c) show a very different irregular surface, deprived of the small craters and with evident dragging marks which could lead to an increase in roughness. Their roughness is similar or even greater than the control paperboard (Table 4). The topographies of the spray-coated samples (4d,e) appear rather different. They also show some signs of dragging but are more homogeneous and have a lower roughness, statistically different from all the others. A smooth-to-the-touch surface guarantees even coverage and is a widely valued characteristic for food packaging materials. These results seem to highlight a higher suitability of the SC technology, properly applied, for achieving homogeneous coatings, because of the small size of droplets deposited on the surface, able to cover any surface irregularities, and the possibility of overcoming the viscosity of the suspension.

4 | Conclusions

When properly applied onto a paperboard substrate, the suspension of MFC/NFC offers a sustainable solution to several critical issues associated with paperboard packaging for dry or fatty foods and non-food products, thanks to the nature of both the coating and the processing methods used.

Although some minor limitations remain regarding interaction with water, due to the inherently hydrophilic nature of cellulose, both the application methods studied allow for the improvement of the characteristics of the basic paperboard, significantly increasing its resistance to grease, without influencing water vapor penetration, and significantly enhancing the barrier to mineral oil hydrocarbons. This last property, in particular, paves the way for a wider use of recycled cellulosic resources, supporting the objectives of the circular economy. Indeed, recycled cellulose, although widely available and inexpensive, is currently underused in packaging due to contamination risk and poor performance. The optimization study has shown that spray coating is the most suitable method for applying the suspension on the paperboards. It allows the use of higher process speeds compatible with industrial production.

It allows the use of higher process speeds compatible with industrial production and allowed achieving the best results in terms of barrier against contaminants and grease resistance.

Given the interesting results and the good lab-scale applicability, the research is moving towards industrialization by studying the coating technologies process applied in industries, also focusing on the study of recycled paper and paperboard in food packaging applications by improving barrier properties and thus reducing the risk of contaminant migration, which is currently a major limitation to the use of recycled cellulose in direct food contact materials.

Author Contributions

Andrea Feroce: data curation, methodology, formal analysis, validation, visualization, writing – original draft, writing – review and editing. **Luciano Piergiovanni:** conceptualization, data curation, methodology, formal analysis, validation, resources, supervision, writing – original draft, writing – review and editing. **Fabio Licciardello:** conceptualization, funding acquisition, resources, project administration, supervision, writing – review and editing.

Acknowledgements

Open access publishing facilitated by Universita degli Studi di Modena e Reggio Emilia, as part of the Wiley - CRUI-CARE agreement.

Conflicts of Interest

The authors declare no conflicts of interest.

Data Availability Statement

The data that support the findings of this study are available from the corresponding author upon reasonable request.

References

1. N. Peelman, P. Ragaert, E. Verguldt, F. Devlieghere, and B. De Meulenaer, "Applicability of biobased packaging materials for long shelf-life food products," *Packaging Research* 1, no. 1 (2016): 7–20.

2. G. K. Deshwal, N. R. Panjagari, and T. Alam, "An overview of paper and paper based food packaging materials: health safety and environmental concerns," *Journal of Food Science and Technology* 56, no. 10 (2019): 4391–4403, https://doi.org/10.1007/s13197-019-03950-z.

3. Mordor Intelligence Research & Advisory. Paper and Paperboard Packaging Market Size, Share, and Growth (2025-2030). Mordor Intelligence. (2024 , December). Retrieved May 7, 2025, from https://www.mordorintelligence.com/industry-reports/global-paper-and-paperboard-packaging-market

4. P. Nechita and M. Roman, "Review on polysaccharides used in coatings for food packaging papers," *Coatings* 10, no. 6 (2020): 566, https://doi.org/10.3390/coatings10060566.

5. Y. F. Chen, T. Liu, L. X. Hu, C. E. Chen, B. Yang, and G. G. Ying, "Unveiling per-and polyfluoroalkyl substance contamination in Chinese paper products and assessing their exposure risk," *Environment International* 185 (2024): 108540, https://doi.org/10.1016/j.envint.2024.108540.

6. P. Miralles, M. I. Beser, Y. Sanchís, V. Yusà, and C. Coscollà, "Determination of 21 per-and poly-fluoroalkyl substances in paper-and cardboard-based food contact materials by ultra-high-performance liquid chromatography coupled to high-resolution mass spectrometry," *Analytical Methods* 15, no. 12 (2023): 1559–1568, https://doi.org/10.1039/D3AY00083D.

7. H. A. Langberg, H. P. H. Arp, G. Castro, A. G. Asimakopoulos, and H. Knutsen, "Recycling of paper, cardboard and its PFAS in Norway,"

Journal of Hazardous Materials Letters 5 (2024): 100096, https://doi.org/10.1016/j.hazl.2023.100096.

8. N. N. Mofokeng, L. M. Madikizela, I. Tiggelman, E. Sanganyado, and L. Chimuka, "Determination of per-and polyfluoroalkyl compounds in paper recycling grades using ultra-high-performance liquid chromatography–high-resolution mass spectrometry," *Environmental Science and Pollution Research* 31, no. 20 (2024): 30126–30136, https://doi.org/10.1007/s11356-024-33250-9.

9. V. Guazzotti, A. Marti, L. Piergiovanni, and S. Limbo, "Bio-based coatings as potential barriers to chemical contaminants from recycled paper and board for food packaging," *Food Additives and Contaminants: Part A* 31, no. 3 (2014): 402–413, https://doi.org/10.1080/19440049.2013.869360.

10. European Commission, "Commission Recommendation (EU) 2017/84 of 16 January 2017 on the monitoring of mineral oil hydrocarbons in food and in materials and articles intended to come into contact with food," *Official Journal of the European Union* 12, no. 84 (2017): 95–96, http://data.europa.eu/eli/reco/2017/84/oj.

11. M. Mujtaba, J. Lipponen, M. Ojanen, S. Puttonen, and H. Vaittinen, "Trends and challenges in the development of bio-based barrier coating materials for paper/cardboard food packaging; a review," *Science of the Total Environment* 851 (2022): 158328, https://doi.org/10.1016/j.scitotenv.2022.158328.

12. P. K. Kunam, D. Ramakanth, K. Akhila, and K. K. Gaikwad, "Bio-based materials for barrier coatings on paper packaging," *Biomass Conversion and Biorefinery* 14, no. 12 (2024): 12637–12652, https://doi.org/10.1007/s13399-022-03241-2.

13. P. Tyagi, K. S. Salem, M. A. Hubbe, and L. Pal, "Advances in barrier coatings and film technologies for achieving sustainable packaging of food products – A review," *Trends in Food Science & Technology* 115 (2021): 461–485, https://doi.org/10.1016/J.TIFS.2021.06.036.

14. S. Agate, P. Tyagi, V. Naithani, L. Lucia, and L. Pal, "Innovating generation of nanocellulose from industrial hemp by dual asymmetric centrifugation," *ACS Sustainable Chemistry & Engineering* 8 (2020): 1850–1858, https://doi.org/10.1021/acssuschemeng.9b05992.

15. S. Singh, G. Şahin, F. A. Silva, et al., "Development of Bio-Based Coatings Incorporating Microfibrillated Cellulose, Lignin and Ionomer Dispersions for Food Contact Applications," *Packaging Technology and Science* (2025), https://doi.org/10.1002/pts.2906.

16. F. Herrick, R. Casebier, J. Hamilton, and K. Sandberg, "Microfibrillated Cellulose: morphology and accessibility," *Journal of Applied Polymer Science: Applied Polymer Symposium* 37 (1983): 797–813.

17. A. Turbak, F. Snyder, and K. Sandberg, "Microfibrillated cellulose, a new cellulose product: properties, uses, and commercial potential," *Journal of Applied Polymer Science: Applied Polymer Symposium* 37 (1983): 815–827.

18. M. Pääkkö, M. Ankerfors, H. Kosonen, et al., "Enzymatic hydrolysis combined with mechanical shearing and high pressure homogenization for nanoscale cellulose fibrils and strong gels," *Biomacromolecules* 8, no. 6 (2007): 1934–1941, https://doi.org/10.1021/bm061215p.

19. M. Henriksson, G. Henriksson, L. A. Berglund, and T. Lindström, "An environmentally friendly method for enzyme-assisted preparation of microfibrillated cellulose (MFC) nanofibers," *European Polymer Journal* 43, no. 8 (2007): 3434–3441, https://doi.org/10.1016/j.eurpolymj.2007.05.038.

20. T. Saito, M. Hirota, N. Tamura, et al., "Individualization of nanosized plant cellulose fibrils by direct surface carboxylation using TEMPO catalyst under neutral conditions," *Biomacromolecules* 10, no. 7 (2009): 1992–1996, https://doi.org/10.1021/bm900414t.

21. T. Saito, Y. Nishiyama, J. L. Putaux, M. Vignon, and A. Isogai, "Homogeneous suspensions of individualized microfibrils from TEMPO-catalyzed oxidation of native cellulose," *Biomacromolecules* 7, no. 6 (2006): 1687–1691, https://doi.org/10.1021/bm060154s.

22. V. Kumar, R. Bollstrom, A. Yang, et al., "Comparison of nano- and microfibrillated cellulose films," *Cellulose* 21, no. 5 (2014): 3443–3456, https://doi.org/10.1007/s10570-014-0357-5.

23. L. Wang, Q. Cui, S. Pan, et al., "Facile isolation of cellulose nanofibers from soybean residue," *Carbohydrate Polymer Technologies and Applications* 2 (2021): 100172, https://doi.org/10.1016/j.carpta.2021.100172.

24. C. N. Schnell, M. C. Inalbon, R. J. Minari, and P. Mocchiutti, "Use of micro/nano-and nanofibrillated cellulose to improve the mechanical properties and wet performance of xylan/chitosan films: A comparison," *ACS Applied Polymer Materials* 5, no. 10 (2023): 7867–7877, https://doi.org/10.1021/acsapm.3c01141.

25. S. Y. Lee, S. J. Chun, I. A. Kang, and J. Y. Park, "Preparation of cellulose nanofibrils by high-pressure homogenizer and cellulose-based composite films," *Journal of Industrial and Engineering Chemistry* 15, no. 1 (2009): 50–55, https://doi.org/10.1016/j.jiec.2008.07.008.

26. T. Taniguchi and K. Okamura, "New films produced from microfibrillated natural fibers," *Polymer International* 47 (1998): 291–294, https://doi.org/10.1002/(SICI)1097-0126(199811)47:3%3C291::AID-PI11%3E3.0.CO;2-1.

27. T. Zimmermann, N. Bordeanu, and E. Strub, "Properties of nanofibrillated cellulose from different raw materials and its reinforcement potential," *Carbohydrate Polymers* 79, no. 4 (2010): 1086–1093, https://doi.org/10.1016/j.carbpol.2009.10.045.

28. D. A. Johnson, M. A. Paradis, M. Bilodeau, B. Crossley, M. Foulger, and P. Gelinas, "Effect of cellulosic nanofibrils on papermaking properties of fines papers," *Tappi Journal* 15, no. 6 (2016): 395–402, https://doi.org/10.32964/TJ15.6.395.

29. M. A. Hubbe, A. Ferrer, P. Tyagi, et al., "Nanocellulose in thin films, coatings, and plies for packaging applications: A review," *BioResources* 12, no. 2017 (2017): 2143–2233.

30. V. Rastogi and P. Samyn, "Bio-based coatings for paper applications," *Coatings* 5 (2015): 887–930, https://doi.org/10.3390/coatings5040887.

31. F. Ansari, Y. Ding, L. A. Berglund, and R. H. Dauskardt, "Toward sustainable multifunctional coatings containing nanocellulose in a hybrid glass matrix," *ACS Nano* 12 (2018): 5495–5503, https://doi.org/10.1021/acsnano.8b01057.

32. H. Zhang, Y. Li, Z. Lu, L. Chen, L. Huang, and M. Fan, "A robust superhydrophobic TiO2NPs coated cellulose sponge for highly efficient oil-water separation," *Nature Scientific Reports* 7 (2017): 3–10, https://doi.org/10.1038/s41598-017-09912-9.

33. S. Yook, H. Park, H. Park, S. Y. Lee, J. Kwon, and H. J. Youn, "Barrier coatings with various types of cellulose nanofibrils and their barrier properties," *Cellulose* 27, no. 8 (2020): 4509–4523, https://doi.org/10.1007/s10570-020-03061-5.

34. F. W. Brodin, Ø. W. Gregersen, and K. Syverud, "Cellulose nanofibrils: Challenges and possibilities as a paper additive or coating material–A review," *Nordic Pulp & Paper Research Journal* 29, no. 1 (2014): 156–166, https://doi.org/10.3183/npprj-2014-29-01-p156-166.

35. A. Adibi, B. M. Trinh, and T. H. Mekonnen, "Recent progress in sustainable barrier paper coating for food packaging applications," *Progress in Organic Coatings* 181 (2023): 107566, https://doi.org/10.1016/j.porgcoat.2023.107566.

36. S. M. M. Mousavi, E. Afra, M. Tajvidi, D. W. Bousfield, and M. Dehghani-Firouzabadi, "Cellulose/carboxymethylcellulose nanofiber blends as efficient coatings to improve the structure and barrier properties of paperboard," *Cellulose* 24 (2017): 3001–3014, https://doi.org/10.1007/s10570-017-1299-5.

37. S. M. M. Mousavi, E. Afra, M. Tajvidi, D. W. Bousfield, and M. Dehghani-Firouzabadi, "Application of cellulose nanofibrils (CNF) as a coating on moderate solids content paperboard at high coating speed using a blade coater," *Progress in Organic Coatings* 122 (2018): 207–218, https://doi.org/10.1016/j.porgcoat.2018.05.024.

38. N. Lavoine, I. Desloges, B. Khelifi, and J. Bras, "Impact of different microfibrillated cellulose coating processes on the mechanical and barrier properties of paper," *Journal of Materials Science* 49 (2014): 2879–2893, https://doi.org/10.1007/s10853-013-7995-0.

39. M. Biedermann, J. E. Ingenhoff, M. Zurfluh, et al., "Migration of mineral oil, photoinitiators and plasticisers from recycled paperboard into dry foods: a study under controlled conditions," *Food Additives and Contaminants: Part A* 30, no. 5 (2013): 885–898, https://doi.org/10.1080/19440049.2013.786189.

40. R. Bandara and G. M. Indunil, "Food packaging from recycled papers: chemical, physical, optical properties and heavy metal migration," *Heliyon* 8, no. 10 (2022), https://doi.org/10.1016/j.heliyon.2022.e10959.

41. AOAC, Association of Official Analytical Chemists, *Official Methods of Analysis*, 16th ed. (, 1995).

42. C. N. Schnell, Q. Tarrés, M. V. Galván, et al., "Polyelectrolyte complexes for assisting the application of lignocellulosic micro/nanofibers in papermaking," *Cellulose* 25 (2018): 6083–6092, https://doi.org/10.1007/s10570-018-1969-y.

43. TAPPI T 559 cm-12. *Grease resistance test for paper and paperboard*. *Technical Association of the Pulp and Paper Industry*, Peachtree Corners, GA, United States, (2012).

44. R. Gaudreault, C. Brochu, R. Sandrock, P. Deglmann, H. Seyffer, and A. Tétreault, "Overview of practical and theoretical aspects of mineral oil contaminants in mill process and paperboard," *Advances in Pulp and Paper Research, Cambridge.* (2013), https://doi.org/10.15376/frc.2013.2.907.

45. TAPPI T 441 OM-9. Water absorptiveness of sized (non-bibulous) paper, paperboard, and corrugated fiberboard (Cobb test). *Technical Association of the Pulp and Paper Industry*, Peachtree Corners, GA, United States, (2013).

46. ASTM. *Standard test methods for water vapor transmission of materials* (E96–00e1) (2001).

47. L. V. Candioti, M. M. De Zan, M. S. Cámara, and H. C. Goicoechea, "Experimental design and multiple response optimization. Using the desirability function in analytical methods development," *Talanta* 124 (2014): 123–138, https://doi.org/10.1016/j.talanta.2014.01.034.

48. K. C. C. C. Benini, H. J. C. Voorwald, M. O. H. Cioffi, M. C. Rezende, and V. Arantes, "Preparation of nanocellulose from Imperata brasiliensis grass using Taguchi method," *Carbohydrate Polymers* 192 (2018): 337–346, https://doi.org/10.1016/j.carbpol.2018.03.055.

49. N. H. Abdul Rahman, B. W. Chieng, N. A. Ibrahim, and R. N. Abdul, "Extraction and characterization of cellulose nanocrystals from tea leaf waste fibers," *Polymers* 9, no. 11 (2017): 588, https://doi.org/10.3390/polym9110588.

50. H. A. Silvério, W. P. Flauzino Neto, N. O. Dantas, and D. Pasquini, "Extraction and characterization of cellulose nanocrystals from corncob for application as reinforcing agent in nanocomposites," *Industrial Crops and Products* 44 (2013): 427–436, https://doi.org/10.1016/j.indcrop.2012.10.014.

51. G. Signori-Iamin, R. J. Aguado, J. L. Putaux, A. F. Santos, W. Thielemans, and M. Delgado-Aguilar, "Energy and property trade-offs in nanocellulose production: High-pressure homogenization at different processing consistencies," *Chemical Engineering Journal* (2025): 161257, https://doi.org/10.1016/j.cej.2025.161257.

52. W. Zhang, G. Zhang, X. A. Lu, J. Wang, and D. Wu, "Cellulosic nanofibers filled poly (β-hydroxybutyrate): Relations between viscoelasticity of composites and aspect ratios of nanofibers," *Carbohydrate Polymers* 265 (2021): 118093, https://doi.org/10.1016/j.carbpol.2021.118093.

53. M. Baalousha and J. Lead, "Rationalizing nanomaterial sizes measured by atomic force microscopy, flow field-flow fractionation, and dynamic light scattering: sample preparation, polydispersity, and particle structure," *Environmental Science & Technology* 46, no. 11 (2012): 6134–6142, https://doi.org/10.1021/es301167x.

54. L. Amoroso, G. Muratore, M. A. Ortenzi, S. Gazzotti, S. Limbo, and L. Piergiovanni, "Fast production of cellulose nanocrystals by hydrolytic-oxidative microwave-assisted treatment," *Polymers* 12, no. 1 (2020): 68, https://doi.org/10.3390/polym12010068.

55. J. Mewis and N. J. Wagner, *Colloidal suspension rheology*, vol. 10 (Cambridge university press, 2012).

56. A. Kroeger, V. Deimede, J. Belack, I. Lieberwirth, G. Fytas, and G. Wegner, "Equilibrium length and shape of rodlike polyelectrolyte micelles in dilute aqueous solutions," *Macromolecules* 40, no. 1 (2007): 105–115, https://doi.org/10.1021/ma061966j.

57. N. Lavoine, J. Bras, and I. Desloges, "Mechanical and barrier properties of cardboard and 3D packaging coated with microfibrillated cellulose," *Journal of Applied Polymer Science* 131, no. 8 (2014), https://doi.org/10.1002/app.40106.

58. N. Ashgriz, ed., *Handbook of atomization and sprays: theory and applications* (Springer Science & Business Media, 2011).

59. K. Shanmugam, S. Varanasi, G. Garnier, and W. Batchelor, "Rapid preparation of smooth nanocellulose films using spray coating," *Cellulose* 24 (2017): 2669–2676, https://doi.org/10.1007/s10570-017-328-4.

60. C. Aulin, M. Gällstedt, and T. Lindström, "Oxygen and oil barrier properties of microfibrillated cellulose films and coatings," *Cellulose* 17 (2010): 559–574, https://doi.org/10.1007/s10570-009-9393-y.

61. E. A. Hassan, M. L. Hassan, R. E. Abou-Zeid, and N. A. El-Wakil, "Novel nanofibrillated cellulose/chitosan nanoparticles nanocomposites films and their use for paper coating," *Industrial Crops and Products* 93 (2016): 219–226, https://doi.org/10.1016/j.indcrop.2015.12.006.

62. J. Zhang, Z. Guo, S. Chen, et al., "High-barrier, strong, and antibacterial paper fabricated by coating acetylated cellulose and cinnamaldehyde for food packaging," *Cellulose* 28 (2021): 4371–4384, https://doi.org/10.1007/s10570-021-03778-x.

63. A. Upadhyay, L. Lucia, and L. Pal, "Functional barrier and recyclable packaging materials through microfibrillated cellulose bilayer composite coatings," *Carbohydrate Polymers* 359 (2025): 123592, https://doi.org/10.1016/j.carbpol.2025.123592.

64. I. Tiggelman, H. Pasch, and P. C. Hartmann, "Rapid comparison of mineral oils vapor transmission rate through paper and board packaging materials," *TAPPI Journal* 2012 (2012), http://hdl.handle.net/10019.1/21851.

65. H. M. Koivula, L. Jalkanen, E. Saukkonen, et al., "Machine-coated starch-based dispersion coatings prevent mineral oil migration from paperboard," *Progress in Organic Coatings* 99 (2016): 173–181, https://doi.org/10.1016/j.porgcoat.2016.05.017.

66. R. Koppolu, G. Banvillet, H. Ghimire, J. Bras, and M. Toivakka, "Enzymatically pretreated high-solid-content nanocellulose for a high-throughput coating process," *ACS Applied Nano Materials* 5, no. 8 (2022): 11302–11313, https://doi.org/10.1021/acsanm.2c02423.

67. G. O'Connor, N. Hudson, and S. Buckley, "Mineral oil barrier testing of cellulose-based and polypropylene-based films," *Packaging Technology and Science* 28, no. 1 (2015): 75–89, https://doi.org/10.1002/pts.2082.

68. J. Brózdowski, J. J. Grkman, T. Kapun, and B. Waliszewska, "Properties of paper coated with Prunus serotina (Ehrh.) extract formulation. *Open*," *Agriculture* 8, no. 1 (2023): 20220189, https://doi.org/10.1515/opag-2022-0189.

69. G. Lavrič, A. Oberlintner, I. Filipova, U. Novak, B. Likozar, and U. Vrabič-Brodnjak, "Functional Nanocellulose, Alginate and Chitosan Nanocomposites Designed as Active Film Packaging Materials," *Polymers* 13, no. 15 (2021): 2523, https://doi.org/10.3390/polym13152523.

70. A. Mayrhofer, S. Kopacic, and W. Bauer, "Extensive Characterization of Alginate, Chitosan and Microfibrillated Cellulose Cast Films to Assess their Suitability as Barrier Coating for Paper and Board," *Polymers* 15, no. 16 (2023): 3336, https://doi.org/10.3390/polym15163336.

71. R. N. Wenzel, "Resistance of solid surfaces to wetting by water," *Industrial and Engineering Chemistry* 28, no. 8 (1936): 988–994, https://doi.org/10.1021/ie50320a024.

72. R. Zhang, Y. Su, and J. Liu, "Different Kinds of Microfibrillated Cellulose as Coating Layers Providing Fiber-based Barrier Properties," *Paper and Biomaterials* 6, no. 1 (2021), https://doi.org/10.12103/j.issn.2096-2355.2021.01.004.

73. S. Huang, X. Wang, Y. Zhang, Y. Meng, F. Hua, and X. Xia, "Cellulose nanofibers/polyvinyl alcohol blends as an efficient coating to improve the hydrophobic and oleophobic properties of paper," *Scientific Reports* 12, no. 1 (2022): 16148, https://doi.org/10.1038/s41598-022-20499-8.

74. N. Lavoine, I. Desloges, B. Manship, and J. Bras, "Antibacterial paperboard packaging using microfibrillated cellulose," *Journal of Food Science and Technology* 52 (2015): 5590–5600, https://doi.org/10.1007/s13197-014-1675-1.

Supporting Information

Additional supporting information can be found online in the Supporting Information section. **Figure S1:** FTIR spectra of suspensions of cellulose fibrils before and after high-pressure homogenization treatment. **Figure S2:** Optical microscopy image of cellulose suspension subjected to high-pressure homogenization. **Figure S3:** a) Water Contact Angle (CA) value; b) and c) Castor oil CA value at time 0 and after 30 second of drop deposition.